Determination of Force and Flux Linkage Characteristics of Radial Active Magnetic Bearings

Boštjan Polajžer[1], Gorazd Štumberger[1], Drago Dolinar[1], and Kay Hameyer[2]
[1]University of Maribor, Faculty of Electrical Engineering and Computer Science
Smetanova 17, 2000 Maribor
Slovenia
email: bostjan.polajzer@uni-mb.si
[2]Katholieke Universiteit Leuven, Department E.E. (ESAT), Division ELECTA
Kasteelpark Arenberg 10, B-3001 Leuven-Heverlee
Belgium

Abstract— **The current and position dependent force and flux linkage characteristics of the studied radial active magnetic bearings are determined by the finite element computations in the entire operating range. Based on results of the performed computations the considerable impact of magnetic nonlinearities and cross coupling effects on properties of radial active magnetic bearings is established. The obtained characteristics are incorporated into the dynamic mathematical model, which is based on the current and position dependent radial forces and partial derivatives of flux linkages.**

Keywords—**Active magnetic bearings, radial force, flux linkage, dynamic mathematical model.**

I. Introduction

ACTIVE magnetic bearings are a system of controlled electromagnets which enable contact-less suspension of a rotor [1]. Two radial bearings and one axial bearing are used to control the five degrees of freedom of the rotor, while an independent driving motor is used to control the sixth degree of freedom. No friction, no lubrication, precise position control and vibration damping make Active Magnetic Bearings (AMB's) particularly appropriate and desirable in high-speed rotating machines. Technical applications include compressors, centrifuges and precise machine tools.

The electromagnets of the discussed radial AMB's (Fig. 1) are placed on the common iron core [2]. Their behavior is therefore magnetically nonlinear. Moreover, the individual electromagnets are magnetically coupled. The impact of magnetic nonlinearities and cross coupling effects on properties of AMB's can be efficiently evaluated in the entire operating range with the analysis of force and flux linkage characteristics.

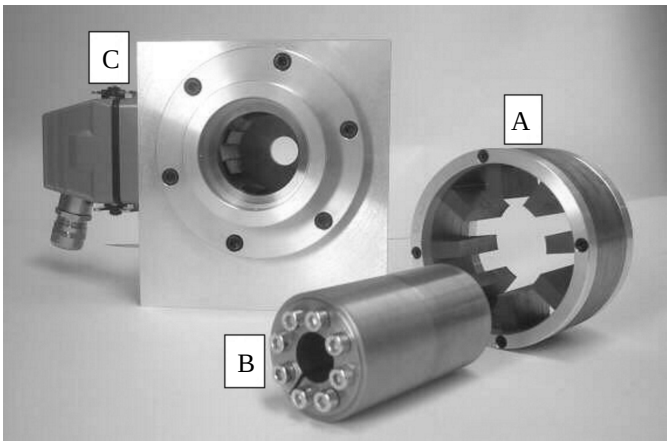

Fig. 1. Radial AMB's: A – stator, B – rotor, C – housing

The force and flux linkage characteristics of the discussed radial AMB's are determined by the Finite Element Method (FEM), using the programming environment described in [3]. The AMB force is calculated by the Maxwell's stress tensor method. The validation of the calculated force is performed through the comparison with the measured force in the entire operating range. Flux linkages are determined from average values of a magnetic vector potential in the coils. The flux linkages was not possible to measure due to the mechanical problems of the rotor fixation. The calculated flux linkage characteristics were therefore examined through the additional force calculation in the entire operating range.

The obtained characteristics are incorporated into the dynamic AMB model, which is based on the current and position dependent radial force and partial derivatives of flux linkages. The presented dynamic model considers the magnetic nonlinearities as well as cross coupling effects, and therefore describes the radial AMB's more complete than dynamic models which are avaliable in the literature [2] [4]. Moreover, it is appropriate for the nonlinear control design, as well as for the real time realization.

II. Finite Element Computation

The geometry and the magnetic field distribution of the discussed radial AMB's is shown in Fig. 2. The problem is formulated by Poisson's equation (1), where $\mathbf{A}$ denotes the magnetic vector potential, ν is the magnetic reluctivity, $\mathbf{J}$ is the current density, and ∇ is Hamilton's differential operator.

$$\nabla \cdot (\nu \nabla \mathbf{A}) = -\mathbf{J} \tag{1}$$

The magneto-static computation was performed by the 2D FEM, using the programming environment described in [3]. In the first step the bearing geometry, the material, the current densities and the boundary conditions were defined. Next, an initial discretization of 9973 nodes and 19824 elements was gen-

0-7803-7763-X/03/$17.00©2003 IEEE

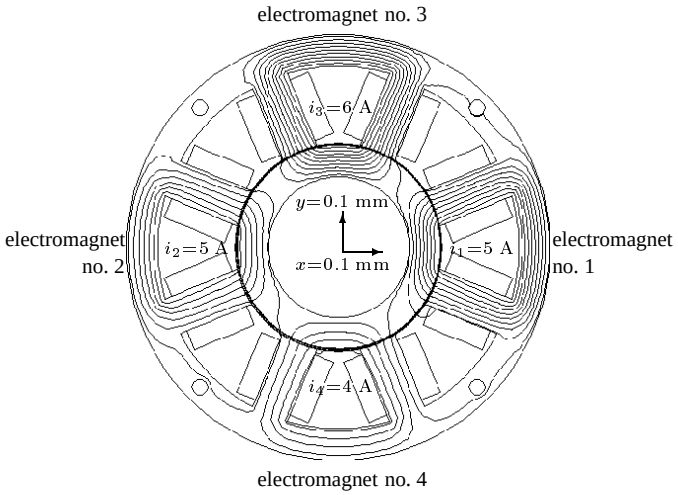

Fig. 2. The Geometry and magnetic field distribution of the discussed radial AMB's for the case $x = y = 0.1$ mm, $i_{x\Delta} = 0$ A, $i_{y\Delta} = 1$ A and $I_0 = 5$ A.

erated. During the analysis of errors, adaptive mesh refinement was applied. Refined mesh is defined by 16442 nodes and 32762 elements, where the value 1.60 for the average aspect ratio is reached.

The radial force characteristics $F_x(i_{x\Delta}, i_{y\Delta}, x, y)$ and $F_y(i_{x\Delta}, i_{y\Delta}, x, y)$ were calculated in the entire operating range using the Maxwell's stress tensor method (2), where l denotes the bearing's axial length, μ_0 the permeability of vacuum, while components of a magnetic flux density are denoted as B_x and B_y. The integration was performed over the contour C placed along the middle layer of the three-layer air gap mesh, shown in Fig. 3a).

$$F_y = \frac{l}{2\mu_0} \oint_C \left(B_y^2 - B_x^2\right) ds \tag{2}$$

The characteristics of flux linkages $\psi_1(i_{x\Delta}, i_{y\Delta}, x, y)$, $\psi_2(i_{x\Delta}, i_{y\Delta}, x, y)$, $\psi_3(i_{x\Delta}, i_{y\Delta}, x, y)$ and $\psi_4(i_{x\Delta}, i_{y\Delta}, x, y)$ were calculated in the entire operating range from average values of the magnetic vector potential in the stator coils (3). N_p denotes the number of turns per pole, while $\bar{A}_{a,k}$, $\bar{A}_{b,k}$, $\bar{A}_{c,k}$ and $\bar{A}_{d,k}$ denote the average values of a magnetic vector potential for the particular coil-end for the k-th electromagnet ($k = 1 \ldots 4$). In Fig. 3b) the magnetic vector potential and the flux linkage of the electromagnet no. 3 is shown.

$$\psi_k = N_p l \left((\bar{A}_{a,k} - \bar{A}_{b,k}) + (\bar{A}_{d,k} - \bar{A}_{c,k}) \right) \tag{3}$$

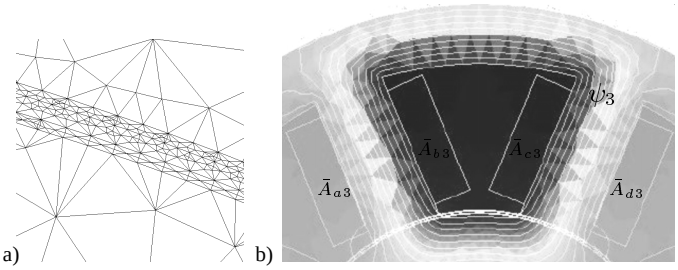

Fig. 3. The refined air gap mesh a), and the magnetic vector potential and the flux linkage of the electromagnet no. 3 b).

Considering the symmetry in geometry (Fig. 2), the mutual influence between electromagnets in the x- axis (no. 1 and no. 2) and electromagnets in the y- axis (no. 3 and no. 4) can be described by (4) and (5).

$$\psi_1(i_{x\Delta}, i_{y\Delta}, x, y) = \psi_2(i_{x\Delta}, i_{y\Delta}, -x, y) \tag{4}$$

$$\psi_3(i_{x\Delta}, i_{y\Delta}, x, y) = \psi_4(i_{x\Delta}, i_{y\Delta}, x, -y) \tag{5}$$

III. Force measurement

Force measurement was performed for different values of the control current and rotor position in the y- axis, while the control current and the rotor position in the x- axis were both equal to zero. The bearing force was measured by a bending beam load cell HBM Z6FC3. The rotor position was measured with an induction proximity probe Vibro-meter TQ401, while a LEM HY 10-P sensor was used for the current measurement. All four electromagnets were supplied by a 20kHz, 270V PWM current source inverter. For the real time feedback algorithm execution and data acquisition a dSPACE 1103 PPC board was used.

IV. Results

Due to the manufacturing process of the rotor steel sheets the magnetic properties of the rotor surface change and the magnetic air gap became larger than the geometric one. The air gap was therefore increased in the FEM-based computations from 0.4 mm to 0.45 mm. The increase in the air gap for 0.05 mm can be compared with the findings in [4].

A good agreement between the radial force characteristics, calculated by the FEM and measured, can be seen in Fig. 4a) and in Fig. 4b). In Fig. 4d) – Fig. 4g) FEM-based results for the flux linkage characteristics are given. Flux linkage characteristics were not measured due to the mechanical problems of the rotor fixation. The calculated flux linkage characteristics were therefore examined through the additional force calculation (6) in the entire operating range. N denotes the total number of turns of the electromagnet and A the area of one pole. α is the force acting angle, while μ_0 and υ denote the permeability of vacuum and the leakage factor respectively. Flux linkage in the y- axis, i.e. ψ_3 and ψ_4 are calculated by the FEM in the entire operating range. Results of the proposed force calculation (6) are shown in Fig. 4c). The agreement between the radial force characteristic calculated by the FEM and calculated by (6) is very good; the maximum relative difference inside the operating range is 10 %.

$$F_y = \frac{\upsilon \cos\alpha}{\mu_0 N^2 A} \left(\psi_3^2 - \psi_4^2\right) \tag{6}$$

To evaluate the impact of magnetic nonlinearities and cross coupling effects on properties of the discussed radial AMB's, it is sufficient to analyze the results inside the operating range ($i_{y\Delta} \in [-2\text{ A}, 2\text{ A}]$, $y \in [-0.1\text{ mm}, 0.1\text{ mm}]$). From the obtained results linear force and flux linkage characteristics of the discussed radial AMB's are determined. However, considering the current and position dependent partial derivatives of flux linkages, the electro motive forces can change considerably due to the magnetic nonlinearities and cross coupling effects.

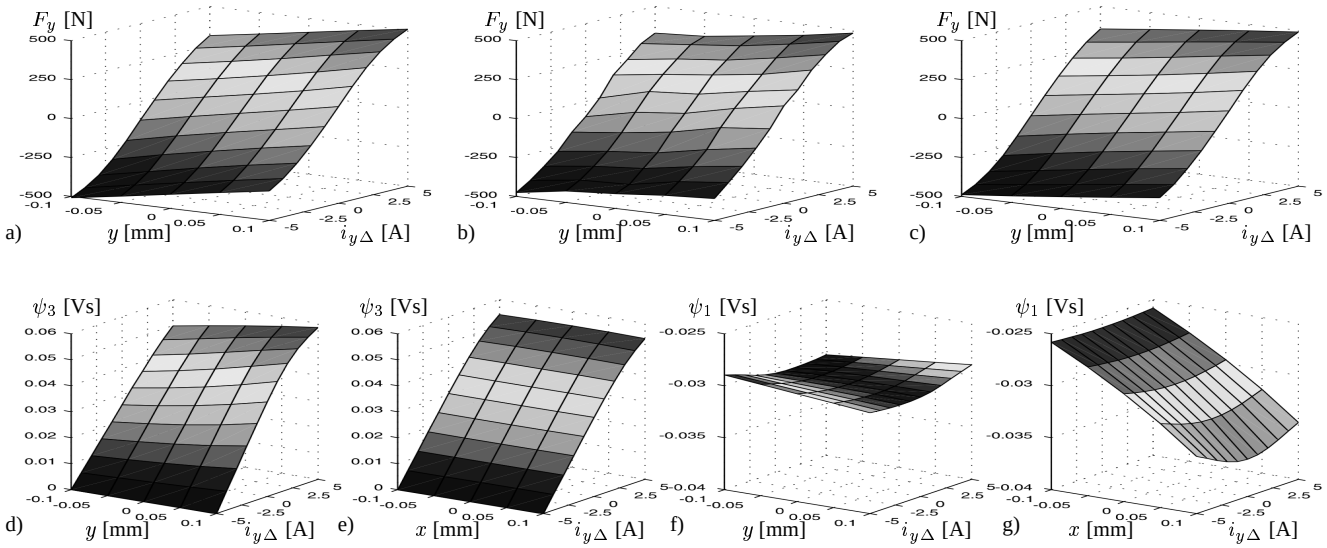

Fig. 4. Radial force characteristic $F_y(i_{y\Delta}, y)$: a) calculated by the FEM, b) measured, c) calculated trough FEM-based flux linkage characteristics. Flux linkage characteristics, calculated by the FEM: d) $\psi_3(i_{y\Delta}, y)$, e) $\psi_3(i_{y\Delta}, x)$, f) $\psi_1(i_{y\Delta}, y)$, g) $\psi_1(i_{y\Delta}, x)$.

V. Dynamic AMB Model

The dynamic AMB model is according to the circuit model presented in Fig. 5 given by (7) and (8):

$$\begin{bmatrix} u_1 \\ u_2 \\ u_3 \\ u_4 \end{bmatrix} = R \begin{bmatrix} I_0 + i_{x\Delta} \\ I_0 - i_{x\Delta} \\ I_0 + i_{y\Delta} \\ I_0 - i_{y\Delta} \end{bmatrix} + 2 \begin{bmatrix} \frac{\partial \psi_1}{\partial i_{x\Delta}} & \frac{\partial \psi_1}{\partial i_{y\Delta}} \\ \frac{\partial \psi_2}{\partial i_{x\Delta}} & \frac{\partial \psi_2}{\partial i_{y\Delta}} \\ \frac{\partial \psi_3}{\partial i_{x\Delta}} & \frac{\partial \psi_3}{\partial i_{y\Delta}} \\ \frac{\partial \psi_4}{\partial i_{x\Delta}} & \frac{\partial \psi_4}{\partial i_{y\Delta}} \end{bmatrix} \begin{bmatrix} \frac{di_{x\Delta}}{dt} \\ \frac{di_{y\Delta}}{dt} \end{bmatrix} + \begin{bmatrix} \frac{\partial \psi_1}{\partial x} & \frac{\partial \psi_1}{\partial y} \\ \frac{\partial \psi_2}{\partial x} & \frac{\partial \psi_2}{\partial y} \\ \frac{\partial \psi_3}{\partial x} & \frac{\partial \psi_3}{\partial y} \\ \frac{\partial \psi_4}{\partial x} & \frac{\partial \psi_4}{\partial y} \end{bmatrix} \begin{bmatrix} \frac{dx}{dt} \\ \frac{dy}{dt} \end{bmatrix} \tag{7}$$

$$\begin{bmatrix} \frac{d^2x}{dt^2} \\ \frac{d^2y}{dt^2} \end{bmatrix} = \frac{1}{m} \begin{bmatrix} F_x(i_{x\Delta}, i_{y\Delta}, x, y) \\ F_y(i_{x\Delta}, i_{y\Delta}, x, y) \end{bmatrix} \tag{8}$$

where u_1, u_2, u_3 and u_4 are the supply voltages, $i_{x\Delta}$ and $i_{y\Delta}$ are the control currents in the x- and in y-axis. R is the coil resistances, m mass of the rotor, while I_0 is the bias current. The FEM-calculated force characteristics $F_x(i_{x\Delta}, i_{y\Delta}, x, y)$ and $F_y(i_{x\Delta}, i_{y\Delta}, x, y)$ and characteristics of flux linkages $\psi_1(i_{x\Delta}, i_{y\Delta}, x, y)$, $\psi_2(i_{x\Delta}, i_{y\Delta}, x, y)$, $\psi_3(i_{x\Delta}, i_{y\Delta}, x, y)$ and $\psi_4(i_{x\Delta}, i_{y\Delta}, x, y)$ are incorporated into the proposed dynamic AMB's model. The current and position dependent partial derivatives of flux linkages required in (7) are calculated through analytical derivations of the continuous approximation functions.

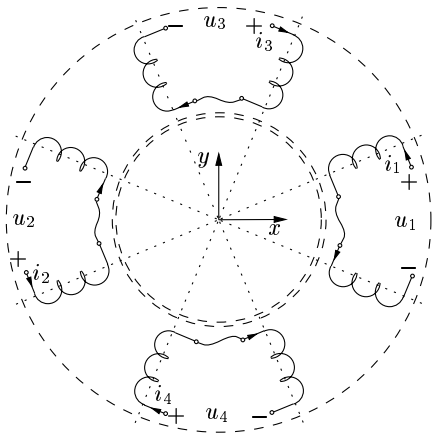

Fig. 5. The circuit AMB model.

VI. Conclusion

The force and flux linkages characteristic of the discussed radial AMB's are determined by the FEM in the entire operating range. The validation of the calculated force is performed through the comparison with the measured force. The measurement of the calculated flux linkages was not performed due to the mechanical problems of the rotor fixation. The calculated flux linkages were therefore examined trough the additional force calculation. It has been shown, that the results of force calculation trough FEM-based flux linkage characteristics are very good. The obtained results show linear force and flux linkage characteristics of the discussed radial AMB's inside the operating range. However, the electro motive forces can change considerably due to the magnetic nonlinearities and cross coupling effects. The obtained characteristics are incorporated into the dynamic AMB model, which is based on the current and position dependent radial force and partial derivatives of flux linkages.

References

[1] G. Schweitzer, H. Bleuler and A. Traxler, *Active magnetic bearings*. ETH Zürich: Vdf Hochschulverlag AG an der ETH Zürich, 1994.

[2] G. Štumberger, D. Dolinar, U. Pahner and K. Hameyer, "Optimization of radial active magnetic bearings using the finite element technique and the differential evolution algorithm," *IEEE Transaction on Magnetics*, vol. 36, no. 4, pp. 1009–1013, 2000.

[3] U. Pahner, R. Mertens, H. De Gersem, R. Belmans, and K. Hameyer, "A parametric finite element environment tuned for numerical optimization," *IEEE Transactions on Magnetics*, vol. 34, no. 5, pp. 2936–2939, 1998.

[4] M. Antila, E. Lantto and A. Arkkio, "Determination of forces and linearized parameters of radial active magnetic bearings by finite element technique," *IEEE Transaction on Magnetics*, vol. 34, no. 3, pp. 684–694, 1998.